AIP Applied Physics Letters

High quality factor nonpolar GaN photonic crystal nanocavities

Tzeng-Tsong Wu, Sheng-Yun Lo, Huei-Min Huang, Che-Wei Tsao, Tien-Chang Lu, and Shing-Chung Wang

Citation: Applied Physics Letters **102**, 191116 (2013); doi: 10.1063/1.4807137
View online: http://dx.doi.org/10.1063/1.4807137
View Table of Contents: http://scitation.aip.org/content/aip/journal/apl/102/19?ver=pdfcov
Published by the AIP Publishing

Articles you may be interested in

High-Q AlN photonic crystal nanobeam cavities fabricated by layer transfer
Appl. Phys. Lett. **101**, 101106 (2012); 10.1063/1.4751336

High quality factor AlN nanocavities embedded in a photonic crystal waveguide
Appl. Phys. Lett. **100**, 191104 (2012); 10.1063/1.4712590

High-Q (>5000) AlN nanobeam photonic crystal cavity embedding GaN quantum dots
Appl. Phys. Lett. **100**, 121103 (2012); 10.1063/1.3695331

High quality factor two dimensional GaN photonic crystal cavity membranes grown on silicon substrate
Appl. Phys. Lett. **100**, 071103 (2012); 10.1063/1.3684630

Reactive ion etching of high optical quality GaNsapphire photonic crystal slab using $CH_4 – H_2$ chemistry
J. Appl. Phys. **101**, 043103 (2007); 10.1063/1.2433770

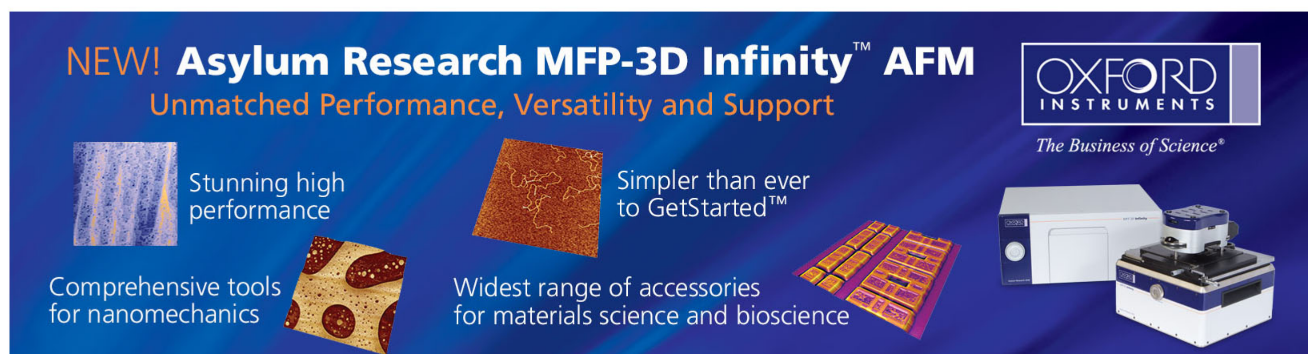

This article is copyrighted as indicated in the article. Reuse of AIP content is subject to the terms at: http://scitation.aip.org/termsconditions. Downloaded to IP: 140.113.38.11 On: Wed, 30 Apr 2014 15:18:05

APPLIED PHYSICS LETTERS **102**, 191116 (2013)

High quality factor nonpolar GaN photonic crystal nanocavities

Tzeng-Tsong Wu, Sheng-Yun Lo, Huei-Min Huang, Che-Wei Tsao, Tien-Chang Lu,[a)] and Shing-Chung Wang
Department of Photonics and Institute of Electro-Optical Engineering, National Chiao Tung University, Hsinchu 30050, Taiwan

(Received 26 March 2013; accepted 3 May 2013; published online 16 May 2013)

High quality factor *a*-plane nonpolar GaN two-dimensional photonic crystal (PC) nanocavities on *r*-plane sapphire substrates have been demonstrated. Nonpolar GaN PC nanocavities on a thin membrane structure were realized by using e-beam lithography to define the PC patterns and focused-ion beam milling to fabricate the suspended thin membrane. A dominant resonant mode at 388 nm with a high quality factor of approximately 4300 has been demonstrated at 77 K by the micro-photoluminescence system. Moreover, the degree of polarization of the emission from the non-polar GaN PC nanocavity was measured to be 64% along the *m* crystalline direction.
© *2013 AIP Publishing LLC*. [http://dx.doi.org/10.1063/1.4807137]

Photonic crystals (PCs), the architecture constructed by periodic index difference materials, have been widely studied and applied to active optoelectronic devices including light emitting diodes (LEDs) and photonic crystal lasers.[1–4] Basically, photonic crystal lasers can be divided into two types including PC band-edge lasers and defect lasers.[5–13] For the PC band-edges lasers, specific Bragg diffractions could be satisfied at the photonic band-edge positions to fulfill laser threshold and surface emitting conditions. So the laser oscillation in a large area can be expected and the high power laser with single mode operation can be realized.[5–11] On the other hand, the PC defect lasers employing the photonic bandgap effect could confine the photons in the defect nanocavities with a thin membrane suspended in the air and achieve a high quality factor with a small mode volume.[12,13] Therefore, the PC defect lasers are potential for development of ultra-low threshold lasers and photonic integrated circuits. In previous literatures, the PC defect lasers were commonly realized in GaAs or InP based material systems because the suspended thin membrane structure which is beneficial to achieve high Q values can be easily made by using selective wet-etching to remove the underneath sacrificial layer.[12,13] On the other hand, fabrication of a thin membrane structure in the GaN-based system is relatively difficult. Several reports have demonstrated GaN-based membrane PC structures by complex etching process of particular epitaxial layers,[14–17] growing nitride-based layers on silicon substrates for selective wet etching,[18,19] and selective thermal decomposition of GaN layers.[20] The quest to demonstrate a GaN-based PC nanocavity is rather intriguing because GaN, such a wide bandgap material, possesses a high exciton binding energy and oscillator strength which is beneficial for supporting high efficiency light emission and exciton-photon coupling capabilities. Especially, nonpolar GaN-based materials have drawn much attention due to the potential for development of high performance light-emitting diodes and lasers.[21–26] The main characteristic of nonpolar GaN is free of polarization fields in the quantum wells which can lead to high internal quantum efficiency and fabrication flexibility.[25,26] Furthermore, nonpolar GaN-based materials can exhibit the anisotropic gain in the *m*-axis or *a*-axis which is beneficial for development of low threshold and high power lasers.[27–29] Since there are no reports of nonpolar GaN PC nanocavities, in this letter, high quality factor nonpolar GaN PC H2 nanocavities have been fabricated and demonstrated. The thin membrane structures were fabricated by focused-ion beam (FIB)[30,31] milling and the PC defect cavities were defined by e-beam lithography (EBL). The resonant mode was observed at 388 nm with a quality factor of approximately 4300 at 77 K. Moreover, the degree of polarization was measured to be 64%. Finally, the numerical calculation results were in a good agreement with the experimental results.

Nonpolar GaN samples were grown on *r*-plane sapphire substrates by the metal-organic chemical vapor deposition (MOCVD) system. The *a*-plane GaN sample structure consisted of an ultrathin SiN_x layer, a 30 nm-thick AlN nucleation layer (NL) and a 2 μm-thick un-doped GaN layer. In the fabrication process, a 300 nm-thick SiN_x layer was deposited by plasma-enhanced chemical vapor deposition (PECVD) on the top of the un-doped GaN layer as the hard mask. Then, a poly-methyl methacrylate (PMMA) photoresist layer was coated on the sample by spin-coating. Subsequently, the PC H2 nanocavities were defined by EBL and the sample was etched approximately 300 nm by reactive ion etching (RIE) down to the SiN_x layer. Then, the PC patterns were etched down to the GaN layer about 300 nm by inductively coupled plasma (ICP) dry etching. Finally, the FIB was utilized to fabricate the thin membrane structure with large air-gap by tilting the sample for ion-beam etching. Fig. 1 shows the scanning electron microscope (SEM) images of the nonpolar GaN PC H2 nanocavities. The number after H means the circle numbers removed from the central photonic crystal lattice. The radius *r*, lattice constant *a* and the *r*/*a* ratio of the PC were measured to be 26.5 nm, 105 nm, and 0.257, respectively. Fig. 1(c) shows the membrane area of nonpolar GaN is estimated to be 10 μm^2. The thickness of the thin membrane layer was measured to be 380 nm.

The photoluminescence (PL) spectra of the fabricated nonpolar GaN PC H2 nanocavities were measured at 77 K. A 325 nm He-Cd continuous wave (CW) laser was used as

[a)]Electronic mail: timtclu@mail.nctu.edu.tw

 © 2013 AIP Publishing LLC

This article is copyrighted as indicated in the article. Reuse of AIP content is subject to the terms at: http://scitation.aip.org/termsconditions. Downloaded to IP: 140.113.38.11 On: Wed, 30 Apr 2014 15:18:05

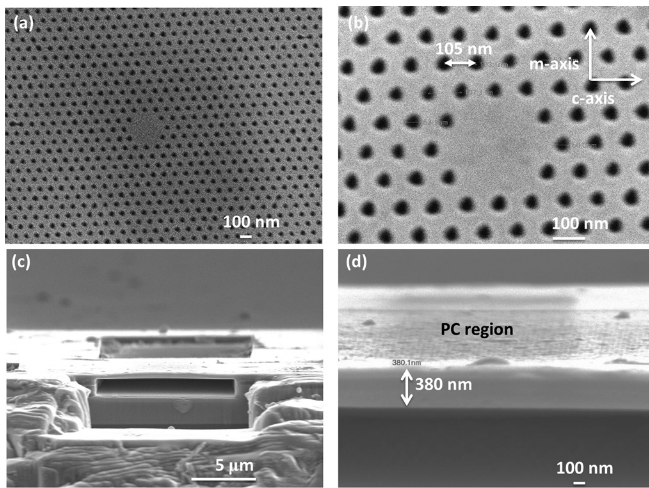

FIG. 1. The SEM images of nonpolar GaN photonic crystal H2 nanocavities for (a) top view, (b) enlarged top view, and (c), (d) tilted angle views of the nonpolar GaN membrane layer. The lattice constant, radius, and thickness of the membrane layer were measured to be 105 nm, 26.5 nm, and 380 nm, respectively.

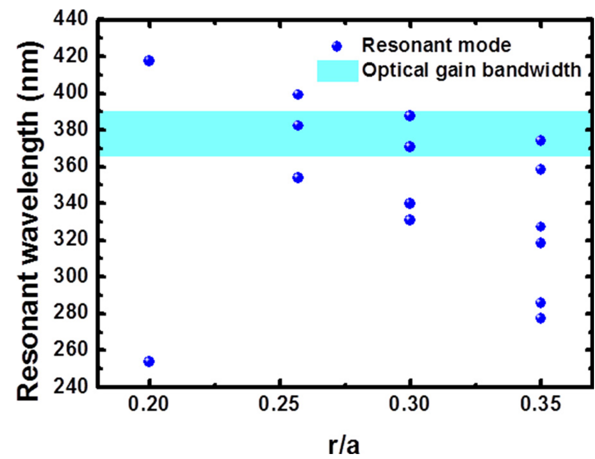

FIG. 3. The *r/a* ratio versus the resonant modes in the nonpolar GaN photonic crystal H2 nanocavities with the same lattice constant of 105 nm. The blue points represent the calculation results by 3D finite difference time domain method. Cyan region shows the optical gain bandwidth of the nonpolar GaN layer.

the optical pumping source. The laser beam with a spot size of about 10 μm to cover the whole PC pattern was obliquely incident onto the devices. The micro-photoluminescence (μ-PL) signal was collected by a 15$\times$ objective lens normal to the sample surface or by a fiber with a 600 μm core in the normal plane of the sample. The collected signal was then fed into a spectrometer (Jobin-Yvon IHR320 Spectrometer) with a spectral resolution about 0.07 nm. The photoluminescence emission peak wavelength of as-grown samples located at 372 nm with a linewidth of about 20 nm measured by the μ-PL system. Using the plane wave expansion method, the corresponding photonic bandgap range of the GaN PC H2 nanocavities can be calculated to be 350 nm to 402 nm which covers the whole emission spectrum of the nonpolar GaN.

Fig. 2 reveals the optical characteristics of the planer sample and nonpolar GaN PC nanocavities in the μ-PL spectra. Compared with the emission spectra of the planer sample, only one resonant mode can be observed at 388 nm locating in the band gap range (350–402 nm) for the nonpolar GaN PC nanocavity sample. In Fig. 2(b), the red curve shows the Lorentz fitting curve of the experimental results. It indicates the linewidth is fitted to be 0.091 nm so that the quality factor can be estimated to be 4300. The high Q factor in the nonpolar GaN PC nanocavities indicates good optical confinement provided by photonic bandgap in the lateral direction and total internal reflection in the vertical direction. Moreover, the quality factor of our nonpolar GaN PC nanocavity is comparable to the previous reports of *c*-plane GaN PC nanocavities, demonstrating that the FIB milling technique is capable to create the smooth surface of the thin membrane layer.

Moreover, the three-dimensional (3D) finite difference time domain (FDTD) method was carried out to calculate the resonant wavelength with respect to the different *r/a* ratio. The simulation parameters such as the lattice constant and radius of PC are extracted from the real devices. Fig. 3 shows the calculation results of the different *r/a* ratio versus the resonant wavelengths. In each r/a, the blue spots represent different resonant mode in H2 nanocavities. The cyan region represents the optical gain band width of the planer nonpolar GaN sample. It can be seen obviously only few number of resonant modes overlapped with the optical gain band width. As the *r/a* ratio is set to be 0.257, the calculation results show only one resonant mode locating at 385 nm in the optical gain spectrum. Compared with the resonant mode observed in the experiment, the calculation result was in a good agreement with the experimental data. On the other hand, the Q factor of the resonant mode at 385 nm with the

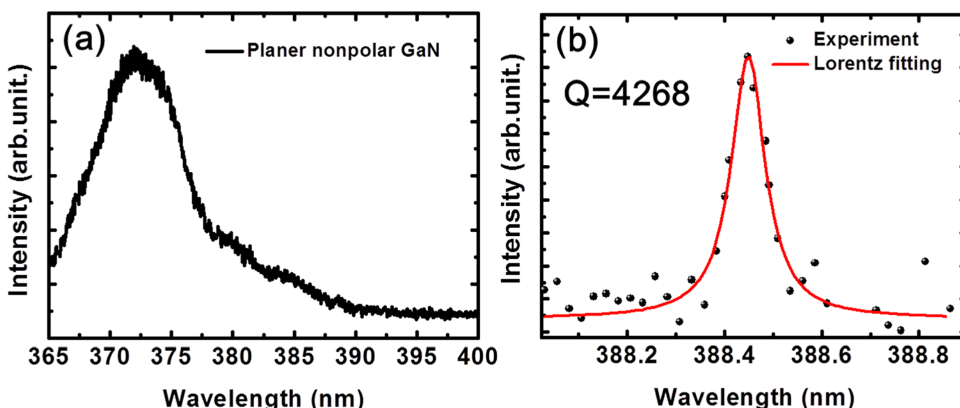

FIG. 2. The micro-PL spectra of (a) the planer nonpolar GaN sample and (b) the nonpolar GaN PC nanocavity at 77 K. The lattice constant and radius of the GaN PC nanocavity were 105 nm and 26.5 nm. Red curve shows the Lorentz fitting result for the measured data points.

This article is copyrighted as indicated in the article. Reuse of AIP content is subject to the terms at: http://scitation.aip.org/termsconditions. Downloaded to IP: 140.113.38.11 On: Wed, 30 Apr 2014 15:18:05

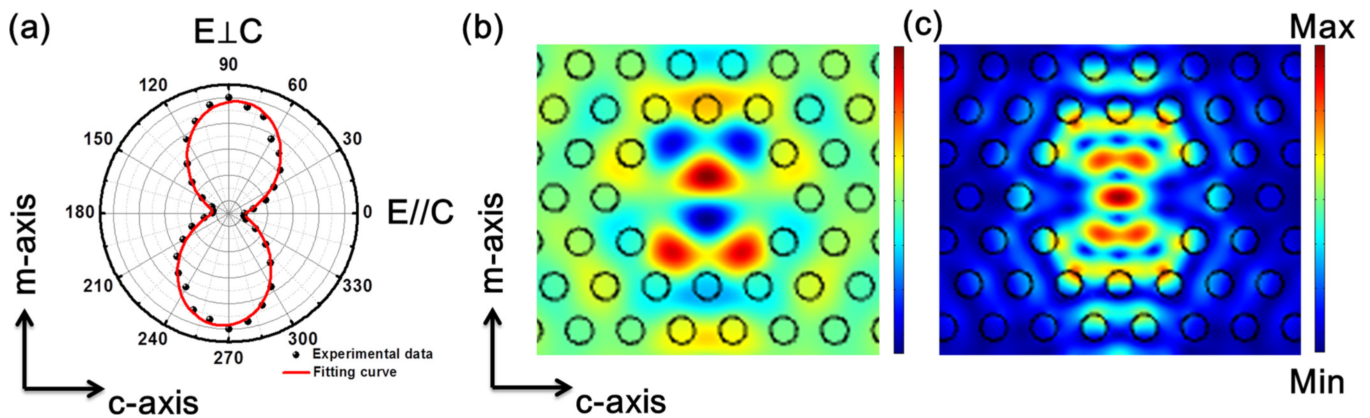

FIG. 4. (a) The polar plot of the resonant peak intensity for the nonpolar GaN PC nanocavity. The degree of polarization was measured to be 64%. (b) The magnetic and (c) square of electric field patterns of the nonpolar GaN PC nanocavity at 385 nm using the 3D finite element method.

same *r*/*a* ratio was calculated by 3D FDTD. The Q factor was calculated to be 1.65×10^4 which was higher than the experimental result. This can be due to the imperfection of the photonic crystal shape in our devices as shown in Fig. 1(b). The other reason is caused by the absorption loss of the GaN layer. In the UV region, the absorption of GaN is around $80\,cm^{-1}$ at 388 nm which is considered the main limitation of the Q factor.[32]

Fig. 4(a) indicates the degree of polarization (DOP) defined as $(I_{max}-I_{min})/(I_{max}+I_{min})$, where I_{max} and I_{min} are the maximum and the minimum intensity of the resonant mode peak. The measured DOP was calculated to be 64% and the polarization direction is along the *m*-axis. Typically, the polarized light can be observed for the *a*-plane GaN due to the fact that the dipole oscillation directions are tend to be perpendicular to the *c*-axis. As a result, the DOP value of the planer nonpolar GaN was measured to be approximately 46%. In order to understand the enhanced DOP value in the PC nanocavities, the 3D finite element method (FEM) was used to calculate the mode pattern at the same resonant wavelength. Fig. 4(b) represents the calculated magnetic field pattern which can be identified as the first order dipole mode. Fig. 4(c) shows the square of electric field pattern in the nonpolar GaN PC nanocavity. The warm and cold colors represent the maximum and minimum value. It can be observed that the strong spot of the electric field is also oscillating along the *m*-axis. The high DOP value of the nonpolar GaN PC nanocavity could be attributed to the specific electric field distribution along the *m*-axis enhancing the dipole oscillation.

In conclusion, high quality factor nonpolar GaN PC H2 nanocavities have been demonstrated. The nonpolar GaN PC H2 nanocavities were fabricated by e-beam lithography and the thin membrane layers were realized by focused-ion beam. In the μ-PL spectra, one resonant mode peak was observed at 388 nm spectra, one resonant mode peak was observed at 388 nm with a high quality factor of approximately 4300 at 77 K. Moreover, the degree of polarization was measured to be 64% due to the specific electric field distribution along the *m*-axis enhancing the dipole oscillation of the nonpolar GaN. The 3D FDTD was carried out for calculation of the resonant wavelength and mode pattern. The calculated results were consisted with experimental results. In the next steps, the lateral p-i-n structure can be utilized in our devices using ion implantation method for realization of the GaN-based electrically pumped PC nanolasers.[33] We believe the presented results would be helpful for development of high efficiency GaN-based light-emitting devices and low threshold PC nanolasers in the near future.

The authors would like to acknowledge Prof. H. C. Kuo at National Chiao Tung University and Dr. Y. J. Cheng at Research Center for Applied Sciences, Academia Sinica for their technical support. This work was supported in part by the Ministry of Education Aim for the Top University program and by the National Science Council of Taiwan under Contract Nos. NSC99-2622-E009-009-CC3 and NSC98-2923-E-009-001-MY3.

[1]E. Yablonovitch, Phys. Rev. Lett. **58**, 2059 (1987).
[2]S. John, Phys. Rev. Lett. **58**, 2486 (1987).
[3]M. Meier, A. Mekis, A. Dodabalapur, A. Timko, R. E. Slusher, J. D. Joannopoulos, and O. Nalamasu, Appl. Phys. Lett. **74**, 7 (1999).
[4]E. Matioli, E. Rangel, M. Iza, B. Fleury, N. Pfaff, J. Speck, E. Hu, and C. Weisbuch, Appl. Phys. Lett. **96**, 031108 (2010).
[5]M. Imada, A. Chutinan, S. Noda, and M. Mochizuki, Phys. Rev. B. **65**, 195306 (2002).
[6]I. Vurgaftman and J. Meyer, IEEE J. Quantum Electron. **39**, 689 (2003).
[7]H. Matsubara, S. Yoshimoto, H. Saito, Y. Jianglin, Y. Tanaka, and S. Noda, Science **319**, 445 (2008).
[8]T. C. Lu, S. W. Chen, L. F. Lin, T. T. Kao, C. C. Kao, P. Yu, H. C. Kuo, S. C. Wang, and S. H. Fan, Appl. Phys. Lett. **92**, 011129 (2008).
[9]S. Kawashima, T. Kawashima, Y. Nagatomo, Y. Hori, H. Iwase, T. Uchida, K. Hoshino, A. Numata, and M. Uchida, Appl. Phys. Lett. **97**, 251112 (2010).
[10]M. Kim, C. S. Kim, W. W. Bewley, J. R. Lindle, C. L. Canedy, I. Vurgaftman, and J. R. Meyer, Appl. Phys. Lett. **88**, 191105 (2006).
[11]L. Sirigu, R. Terazzi, I. Amanti, M. Giovannini, J. Faist, A. Dunbar, and R. Houdré, Opt. Express **16**, 5206 (2008).
[12]O. Painter, R. K. Lee, A. Scherer, A. Yariv, J. D. O'Brien, P. D. Dapkus, and I. Kim, Science **284**, 1819 (1999).
[13]H. G. Park, S. H. Kim, S. H. Kwon, Y. Ju, J. K. Yang, J. H. Baek, S. B. Kim, and Y. H. Lee, Science **305**, 1444 (2004).
[14]Y.-S. Choi, K. Hennessy, R. Sharma, E. Haberer, Y. Gao, S. P. DenBaars, S. Nakamura, and E. L. Hu, Appl. Phys. Lett. **87**, 243101 (2005).
[15]M. Arita, S. Ishida, S. Kako, S. Iwamoto, and Y. Arakawa, Appl. Phys. Lett. **91**, 051106 (2007).
[16]C. H. Lin, J. Y. Wang, C. Y. Chen, K. C. Shen, D. M. Yeh, Y. W. Kiang, and C. Yang, Nanotechnology **22**, 025201 (2011).
[17]D. U. Kim, S. Kim, J. Lee, S. R. Jeon, and H. Jeon, IEEE Photon. Technol. Lett. **23**, 1454 (2011).

This article is copyrighted as indicated in the article. Reuse of AIP content is subject to the terms at: http://scitation.aip.org/termsconditions. Downloaded to IP: 140.113.38.11 On: Wed, 30 Apr 2014 15:18:05

[18]D. NeôČel, S. Sergent, M. Mexis, D. Sam-Giao, T. Guillet, C. Brimont, T. Bretagnon, F. Semond, B. Gayral, S. David, X. Checoury, and P. Boucaud, Appl. Phys. Lett. **98**, 261106 (2011).
[19]N. Vico Triviño, G. Rossbach, U. Dharanipathy, J. Levrat, A. Castiglia, J.-F. Carlin, K. A. Atlasov, R. Butté, R. Houdré, and N. Grandjean, Appl. Phys. Lett. **100**, 071103 (2012).
[20]M. Arita, S. Kako, S. Iwamoto, and Y. Arakawa, Appl. Phys. Express **5**, 126502 (2012).
[21]M. Craven, S. H. Lim, F. Wu, J. S. Speck, and S. P. DenBaars, Appl. Phys. Lett. **81**, 469 (2002).
[22]B. Haskell, F. Wu, S. Matsuda, M. D. Craven, P. T. Fini, S. P. Denbaars, J. S. Speck, and S. Nakamura, Appl. Phys. Lett. **83**, 1554 (2003).
[23]P. Waltereit, O. Brandt, M. Ramsteiner, A. Trampert, H. T. Grahn, J. Menniger, M. Reiche, R. Uecker, P. Reiche, and K. H. Ploog, Phys. Status Solidi A **180**, 133 (2000).
[24]C. Holder, J. S. Speck, S. P. DenBaars, S. Nakamura, and D. Feezell, Appl. Phys. Express **5**, 092104 (2012).
[25]P. Waltereit, O. Brandt, M. Ramsteiner, A. Trampert, H. T. Grahn, J. Menniger, M. Reiche, R. Uecker, P. Reiche, and K. H. Ploog, Nature **406**, 865 (2000).
[26]C. Y. Chang, H. M. Huang, C. M. Lai, and T. C. Lu, IEEE J. Quantum Electron. **48**, 867 (2012).
[27]T. Ohtoshi, A. Niwa, and T. Kuroda, J. Appl. Phys. **82**, 1518 (1997).
[28]W. Scheibenzuber, U. Schwarz, R. Veprek, B. Witzigmann, and A. Hangleiter, Phys. Rev. B **80**, 115320 (2009).
[29]S. Takigawa and S. Noda, Opt. Express **19**, 9475 (2011).
[30]T. M. Babinec, J. T. Choy, K. J. M. Smith, M. Khan, and M. Lončar, J. Vac. Sci. Technol. B **29**, 010601 (2011).
[31]T. T. Wu, Y. C. Syu, S. H. Wu, W. T. Chen, T. C. Lu, S. C. Wang, H. P. Chiang, and D. P. Tsai, Opt. Express **20**, 20551 (2012).
[32]F. Omnès, N. Marenco, B. Beaumont, Ph. de Mierry, E. Monroy, F. Calle, and E. Muñoz, J. Appl. Phys. **86**, 5286 (1999).
[33]B. Ellis, T. Sarmiento, M. Mayer, B. Zhang, J. Harris, E. Haller, and J. Vuckovic, Appl. Phys. Lett. **96**, 181103 (2010).

This article is copyrighted as indicated in the article. Reuse of AIP content is subject to the terms at: http://scitation.aip.org/termsconditions. Downloaded to IP: 140.113.38.11 On: Wed, 30 Apr 2014 15:18:05